CrystEngComm

ROYAL SOCIETY OF CHEMISTRY

COMMUNICATION

View Article Online
View Journal | View Issue

Check for updates

Cite this: *CrystEngComm*, 2020, **22**, 5573

Received 22nd July 2020,
Accepted 8th August 2020

DOI: 10.1039/d0ce01065k

rsc.li/crystengcomm

Published on 10 agosto 2020. Downloaded on 09/10/2024 05:17:54.

Halogen-bonded cocrystals of donepezil with perfluorinated diiodobenzenes†

Vinko Nemec, [a] Toni Vitasović [ab] and Dominik Cinčić *[a]

Donepezil, an active pharmaceutical ingredient with several different acceptor sites for halogen bonding has successfully been cocrystallized with two perfluorinated halogen bond donors. The prepared cocrystals provide insight into the halogen bonding potential of organic molecules with increased structural complexity.

Donepezil (**dpz**) is an active pharmaceutical ingredient (API) that is usually taken in the form of its chloride salt as a drug for relieving symptoms of Alzheimer's disease.[1] To that end, most patents and research on crystal engineering of **dpz** systems, including the recent study by Lee and coworkers,[2] have been focused on chloride salts, polymorphism and hydrogen bonded cocrystals, primarily with organic acids.[3] On the other hand, searching for "donepezil cocrystal" or "donepezil co-crystal" resulted in only one match[4] in the patent databases used.[5] In the CSD (Cambridge Structural Database),[6] the donepezil molecule is present in 16 datasets. Six of those correspond to different polymorphs of **dpz**,[7] one dataset corresponds to a hydrate[2] and the remaining nine are salts or salt solvates with: fumaric acid (refcode IGIWON),[2] mandelic acid (solvate refcode IGIWUT, hemihydrate refcode IGIXEE),[2] maleic acid (refcode IGIXAA),[2] methanesulfonic acid (refcode KUTQAT),[8] benzenesulfonic acid (refcode KUTPUM, hydrate refcode IGOCIT),[2,8] *p*-toluenesulfonic acid (refcode KUTPOG),[8] and oxalic acid (trihydrate refcode XETKEN).[3b]

From the point of view of crystal engineering multi-component halogen-bonded materials,[9] **dpz** as a molecule presents an interesting multiacceptor target, since it contains the following species that are potential halogen bond[10] acceptors: a) carbonyl oxygen atom,[11] b) piperidinyl nitrogen atom,[12] c) two methoxy oxygen atoms in close proximity, such that they can act as either separate acceptors, or as acceptors of a bifurcated I···$(O_{methoxy})_2$ halogen bond,[13,14] and d) two aromatic ring systems[15] (Scheme 1). Additionally, **dpz** in its unprotonated form lacks strong hydrogen bond donor atoms, so it can be expected that there will be no competition between halogen bonds and potentially weak hydrogen bonds, *e.g.*, C–H···O or C–H···N. In our work, we selected perfluorinated diiodobenzenes as cocrystal coformers for **dpz** (Scheme 1): 1,4-diiodotetrafluorobenzene (**14tfib**) and 1,3-diiodotetrafluorobenzene (**13tfib**). Both selected isomers are potential ditopic halogen bond donors that differ in their ability to form halogen-bonded cocrystals.[16]

Cocrystal screening was performed by mechanochemical means, by liquid-assisted grinding (LAG)[17] of reaction mixtures with 1 : 1 and 1 : 2 reactant stoichiometry (**dpz** : donor). Milling was conducted in a Retsch MM200 mill using stainless steel jars under normal laboratory conditions (temperature *ca.* 25 °C, 40–60% relative humidity, see ESI†).

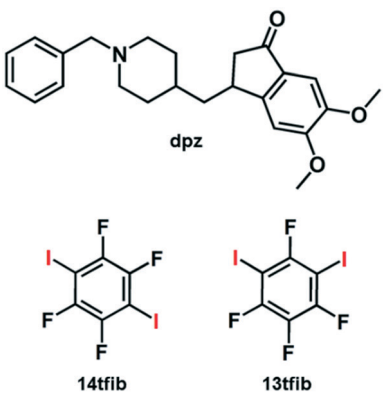

Scheme 1 Molecular structure of donepezil and halogen bond donors used in this study.

[a] *Department of Chemistry, Faculty of Science, University of Zagreb, Horvatovac 102a, HR-10002 Zagreb, Croatia. E-mail: dominik@chem.pmf.hr*
[b] *Interdisciplinary Nanoscience Center (iNANO), Aarhus University, Gustav Wieds Vej 14, DK-8000 Aarhus C, Denmark*

† Electronic supplementary information (ESI) available: Synthetic details, single crystal and powder X-ray diffraction data. CCDC 2017056 and 2017057 contain crystallographic data for this paper. For ESI and crystallographic data in CIF or other electronic format see DOI: 10.1039/d0ce01065k

Published on 10 agosto 2020. Downloaded on 09/10/2024 05:17:54.

The reactants and products were then characterized by powder X-ray diffraction (PXRD) and differential scanning calorimetry (DSC). In order to structurally characterize the new products, mechanochemical experiments were followed by solution crystallization experiments, by dissolving the reactants in an appropriate solvent with heating, followed by letting the obtained solution cool down and evaporate at room temperature (see ESI†). The obtained products were then structurally characterized by single crystal X-ray diffraction (SCXRD).

Mechanochemical screening experiments have shown that new products are formed by milling **dpz** with **13tfib** or **14tfib**. Single crystals were obtained for both new products, and structural analysis revealed that their formulas are: (**dpz**)(**13tfib**) and (**dpz**)(**14tfib**)$_2$. The measured PXRD patterns for the mechanochemical products were found to be in good agreement with the patterns calculated from single crystal data (Fig. 1), and the DSC experiments show that both cocrystals were obtained as pure single phases (see ESI†).

Molecular and crystal structure determination based on single crystal X-ray diffraction has revealed that I···N and I···O halogen bonds are present in both cocrystals. As expected, both **13tfib** and **14tfib** molecules act as ditopic halogen bond donors. In the (**dpz**)(**13tfib**) cocrystal, each **dpz** molecule participates in halogen bonding with **13tfib** *via* I···N and I···O$_{carbonyl}$ halogen bonds (Table 1). This results in the formation of discrete four-membered halogen-bonded assemblies (Fig. 2a). The two methoxy oxygen atoms of **dpz** do not participate in the formation of either hydrogen or halogen bonds – they are instead "blocked off" by the close packing of the pendant benzyl fragment belonging to an adjacent **dpz** molecule. The four-membered complexes are connected into chains by C–H···F contacts (d(C29···F4) = 3.53(1) Å) that are further interconnected in 3D *via* C–H···F (d(C8···F1) = 3.327(9) Å, d(C19A···F1) = 3.52(1) Å, d(C20B···F1) = 3.48(3) Å) and C–H···C (d(C18···C6) = 3.646(9) Å, d(C20A···C24) = 3.53(2) Å) contacts.

Similarly, both the piperidinyl nitrogen and carbonyl oxygen atom participate in halogen bonding in the (**dpz**)(**14tfib**)$_2$ cocrystal (Fig. 2b). However, each **dpz** molecule in this system participates in halogen bonding with three crystallographically independent **14tfib** molecules, in such a way that the carbonyl oxygen atom functions as a bifurcated halogen bond acceptor, participating in I···O$_{carbonyl}$ halogen bonds with two **14tfib** molecules (Table 1). All three crystallographically independent **14tfib** molecules exhibit different supramolecular bonding. The first **14tfib** molecule is a ditopic halogen bond donor that connects two **dpz** molecules *via* I···O$_{carbonyl}$ halogen bonds. In the second crystallographically independent **14tfib** molecule one iodine atom participates in I···O$_{carbonyl}$ halogen bonding with **dpz**, while the other iodine atom is enveloped by the piperidinyl and benzyl fragments of another **dpz** molecule. The third crystallographically independent **14tfib** molecule is a ditopic halogen bond donor that connects two **dpz** molecules *via* I···N halogen bonds. The resulting combination of halogen bonds leads to the formation of an intricate molecular chain. Halogen bonding parameters are listed in Table 1. In contrast to the (**dpz**)(**13tfib**) cocrystal, in the (**dpz**)(**14tfib**)$_2$ cocrystal methoxy oxygen atoms participate in hydrogen bonding, forming an $R_2^4(12)$ supramolecular motif (d(C35···O2) =

Table 1 Halogen bond lengths (d), angles (∠) and relative shortenings (*R.S.*) of D···A distances in the herein prepared cocrystals

Cocrystal	D···A	d(D···A)/Å	*R.S.*[a]/%	∠(C–D···A)/°
(**dpz**)(**13tfib**)	I1···N1	2.833(4)	19.7	177.1(2)
	I2···O1	3.003(5)	14.2	174.3(2)
(**dpz**)(**14tfib**)$_2$	I1···N1	2.910(8)	17.5	173.8(3)
	I2···O1	3.250(9)	7.1	174.9(3)
	I3···O1	3.007(8)	14.1	177.9(4)

[a] $R.S. = 1 - d(D\cdots A)/[r_{vdW}(D) + r_{vdW}(A)]$.[18]

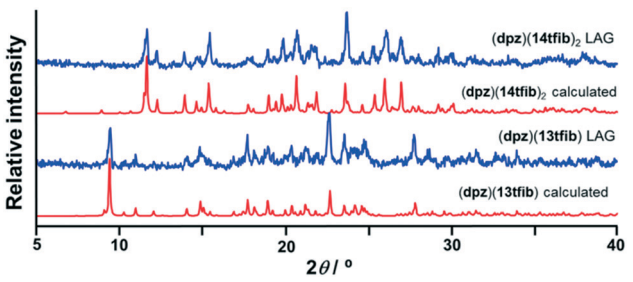

Fig. 1 Comparison of experimental powder patterns obtained by LAG with those generated from single crystal data.

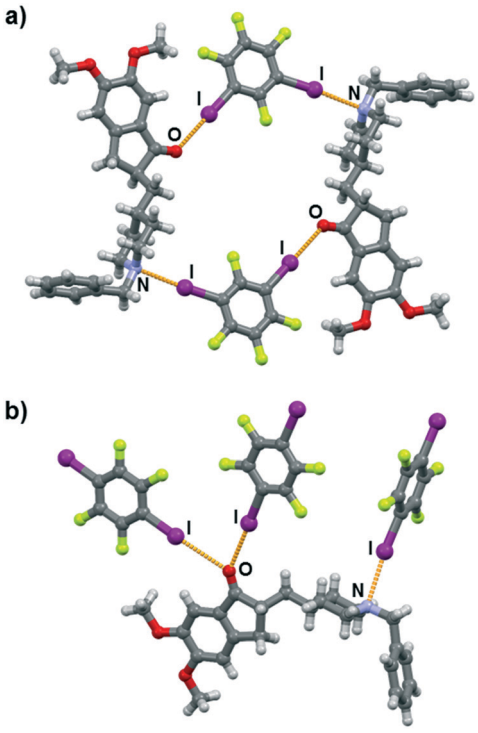

Fig. 2 Parts of the crystal structure in a) (**dpz**)(**13tfib**) and b) (**dpz**)(**14tfib**)$_2$. Enantiomeric disorder is removed for clarity (the position of two C atoms and their riding H atoms). Halogen bonds are coloured orange.

 This journal is © The Royal Society of Chemistry 2020

Published on 10 agosto 2020. Downloaded on 09/10/2024 05:17:54.

3.32(2) Å, ∠(C35–H35A···O2) = 128°, *d*(C35···O3) = 3.52(2) Å, ∠(C35–H35A···O3) = 158°), and in combination with the above-mentioned halogen bonding lead to the formation of a 2D network. Numerous C–H···F interactions are present in the network (*d*(C15···F2) = 3.14(2) Å, *d*(C16···F2) = 3.14(2) Å, *d*(C32···F6) = 3.40(2) Å, *d*(C36···F4) = 3.36(1) Å), and also assist in network stacking into 3D (*d*(C20···F1) = 3.17(1) Å).

While the halogen bond dataset obtained in this work is statistically small, it mostly fits previous observations. Halogen bonds with piperidinyl nitrogen atoms in these cocrystals are mostly linear and have a large value of donor···acceptor distance shortening (*R.S.*) with respect to the sum of van der Waals radii[18] that is comparable to well-researched halogen bonds with pyridyl nitrogen atoms.[9a,19]

Halogen bonds with carbonyl oxygen atoms are also quite linear but have a slightly smaller value of *R.S.* The one exception is the halogen bond with the bridging **14tfib** molecule (I2···O1) where this value drops down to only 7.1%, which is comparable to weaker Br···O halogen bonds with carbonyl oxygen atoms.[20] This can be ascribed to supramolecular packing effects in the (**dpz**)(**14tfib**)$_2$ structure coupled with acceptor strength. The carbonyl oxygen atom in question is a simultaneous acceptor of two halogen bonds, meaning that it can participate in halogen bonding in two ways: by forming two bonds of relatively equal strength, or by forming one stronger and one weaker bond. Since the non-bridging **14tfib** molecule has to fill in the space enveloped by another **dpz** molecule, it is sterically advantageous for it to form a strong halogen bond. As a result, the oxygen atom weakens as an acceptor in the direction of the bridging **14tfib** molecule, which leads to a sterically favorable lengthening of the halogen bond (Fig. 3b). Furthermore, the bridging molecule participates in two halogen bonds with oxygen atoms on two **dpz** molecules and in supramolecular interactions with nearby weak hydrogen bond donors, meaning that weakening of these individual halogen bonds probably has less of an effect on structural stability than if the bond with the non-bridging molecule were weakened.

Thermal analysis experiments (see ESI†) have shown that both prepared cocrystals have similar thermal stabilities. Their DSC curves exhibit one, well-defined, endothermic peak which corresponds to melting, at 113 °C for (**dpz**)(**13tfib**) and 111 °C for (**dpz**)(**14tfib**)$_2$. Their melting points are *ca.* 20 °C higher than that of the pure **dpz** (91 °C). The similarity in thermal degradation temperature is interesting, considering their different stoichiometries and supramolecular architectures, as well as the fact that the pure halogen bond donors, **13tfib** and **14tfib**, have a melting point of 23 °C and 108 °C, respectively.

To conclude, our cocrystallization experiments have resulted in two new halogen-bonded cocrystals with the selected API molecule. In line with our previous work, the carbonyl oxygen atom has proven its potential as a good halogen bond acceptor, along with the piperidinyl nitrogen atom, even if they are present in a bulkier molecule such as **dpz**, which contains a larger variety of functional groups that are potential acceptor sites. Furthermore, the carbonyl oxygen atom as both a monocentric or bifurcated halogen bond acceptor species turned out to be competitive with the piperidinyl nitrogen atom. In keeping with previous comparisons of **13tfib** and **14tfib** cocrystals, this work reveals similarities in halogen bond lengths and melting points of their cocrystals,[16] as well as differences in stoichiometric compositions of cocrystals and the underlying halogen bonding motifs. Finally, we believe that the described results are important in the context of crystal engineering of pharmaceutical materials and in tuning API solid state properties. Further research into halogen bonding might allow for the design of new families of halogen bond donors which could then be used as appropriate coformers in future pharmaceutical cocrystals.

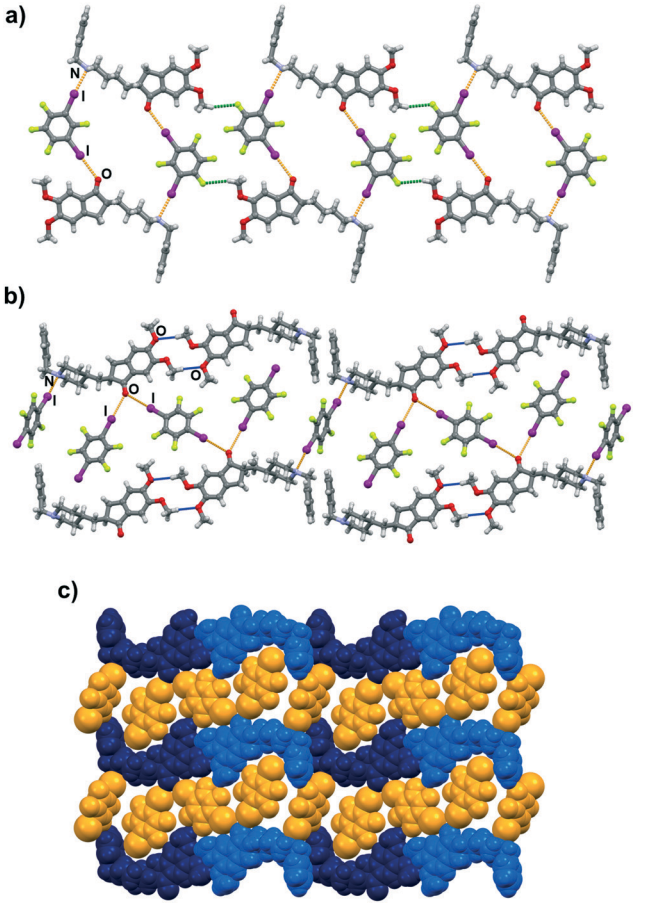

Fig. 3 Parts of the crystal structure of: a) (**dpz**)(**13tfib**), b) (**dpz**)(**14tfib**)$_2$ showcasing the supramolecular connectivity in a layer. c) Spacefill view of a part of the crystal structure in (**dpz**)(**14tfib**)$_2$. Enantiomeric disorder is removed for clarity (the position of two C atoms and their riding H atoms). Halogen bonds are coloured orange, C–H···F contacts are coloured green and C–H···O hydrogen bonds are coloured blue.

Conflicts of interest

There are no conflicts to declare.

Published on 10 agosto 2020. Downloaded on 09/10/2024 05:17:54.

Acknowledgements

This research was supported by the Croatian Science Foundation under the projects IP-2014-09-7367 and IP-2019-04-1868.

Notes and references

1 (*a*) H. Sugimoto, H. Ogura, Y. Arai, Y. Iimura and Y. Yamanishi, *Jpn. J. Pharmacol.*, 2002, **89**, 7–20; (*b*) B. Seltzer, *Expert Opin. Drug Metab. Toxicol.*, 2005, **1**, 527–536; (*c*) M. P. Murphy and H. LeVine, *J. Alzheimer's Dis.*, 2010, **19**, 311–323.

2 J. H. Bae, H. J. Sun, A. Park, D. Kim, J. Yeon, S. K. Kang and E. H. Lee, *Cryst. Growth Des.*, 2020, **20**, 2283–2293.

3 (*a*) T. B. Patel, T. R. Patel and B. N. Suhagia, *Int. J. Pharma Sci. Res.*, 2016, **7**, 2097–2108; (*b*) K. Ravikumar, B. Sridhar, D. G. Sathe, A. V. Naidu and K. D. Sawant, *Acta Crystallogr., Sect. C: Cryst. Struct. Commun.*, 2006, **62**(2006), o681–o683; (*c*) W. Somphon, A. Prasertsabw and N. Jarussophon, *Mater. Today: Proc.*, 2019, **17**, 1887–1897; (*d*) A. Manikowski, B. Ziobro, A. Zaba, M. Makosza, J. Jerkovic, I. Grebenar, E. Mestrovic, Z. M. Samardzic, L. Lerman and K. Kaczorowska, WO2007/015052A1, 2007; (*e*) T. Mezei, G. Simig, G. Lukács, M. Porcs-Makkay, B. Volk, E. Molnár and V. Hofmanné Fekete, WO2006/030249A1, 2006.

4 T. H. Zhang, EP2204364A1, 2010.

5 (*a*) http://www.uspto.gov/ (search date March 30th, 2020); (*b*) https://worldwide.espacenet.com/patent/ (search date March 30th, 2020); (*c*) https://www.j-platpat.inpit.go.jp/ (search date March 30th, 2020).

6 C. R. Groom, I. J. Bruno, M. P. Lightfoot and S. C. Ward, *Acta Crystallogr., Sect. B: Struct. Sci., Cryst. Eng. Mater.*, 2016, **72**, 171–179.

7 (*a*) M. G. Cardozo, T. Kawai, Y. Iimura, H. Sugimoto, Y. Yamanishi and A. J. Hopfinger, *J. Med. Chem.*, 1992, **35**, 590–601; (*b*) Y. Park, J. Lee, S. H. Lee, H. G. Choi, C. Mao, S. K. Kang, S.-E. Choi and E. H. Lee, *Cryst. Growth Des.*, 2013, **13**, 5450–5458; (*c*) Y. Park, S. X. M. Boerrigter, J. Yeon, S. H. Lee, S. K. Kang and E. H. Lee, *Cryst. Growth Des.*, 2016, **16**, 2552–2560.

8 S. H. Lee, J. H. Bae, Y. Park, B. R. Adhikari, C. Mao, D. Kim, K. I. Kim, S. K. Kang and E. H. Lee, *Cryst. Growth Des.*, 2015, **15**, 3123–3130.

9 (*a*) G. Cavallo, P. Metrangolo, R. Milani, T. Pilati, A. Priimagi, G. Resnati and G. Terraneo, *Chem. Rev.*, 2016, **116**, 2478–2601; (*b*) R. W. Troff, T. Mäkelä, F. Topić, A. Valkonen, K. Raatikainen and K. Rissanen, *Eur. J. Org. Chem.*, 2013, 1617; (*c*) D. Yan, A. Delori, G. O. Lloyd, T. Friščić, G. M. Day, W. Jones, J. Lu, M. Wei, D. G. Evans and X. Duan, *Angew. Chem., Int. Ed.*, 2011, **50**, 12483; (*d*) M. A. Sinwell and L. R. MacGillivray, *Angew. Chem., Int. Ed.*, 2016, **55**, 3477; (*e*) O. S. Bushuyev, T. Friščić and C. J. Barrett, *Cryst. Growth Des.*, 2016, **16**, 541.

10 (*a*) A. Priimagi, G. Cavallo, P. Metrangolo and G. Resnati, *Acc. Chem. Res.*, 2013, **46**, 2686; (*b*) G. R. Desiraju, P. Shing Ho, L. Kloo, A. C. Legon, R. Marquardt, P. Metrangolo, P. Politzer, G. Resnati and K. Rissanen, *Pure Appl. Chem.*, 2013, **85**, 1711.

11 (*a*) J.-L. Syssa-Magalé, K. Boubeker and B. Schöllhorn, *J. Mol. Struct.*, 2005, **737**, 103–107; (*b*) M. Zbačnik, M. Pajski, V. Stilinović, M. Vitković and D. Cinčić, *CrystEngComm*, 2017, **19**, 5576–5582; (*c*) D. Cinčić and T. Friščić, *CrystEngComm*, 2014, **16**, 10169–10172; (*d*) V. Nemec and D. Cinčić, *CrystEngComm*, 2016, **18**, 7425–7429; (*e*) G. Bergamaschi, L. Lascialfari, A. Pizzi, M. I. Martinez Espinoza, N. Demitri, A. Milani, A. Gori and P. Metrangolo, *Chem. Commun.*, 2018, **54**, 10718–10721; (*f*) V. Nemec, L. Fotović, T. Vitasović and D. Cinčić, *CrystEngComm*, 2019, **21**, 3251–3255; (*g*) X.-Q. Yang, Z.-Y. Yi, S.-F. Wang, T. Chen and D. Wang, *Chem. Commun.*, 2020, **56**, 3539.

12 (*a*) D. Cinčić, T. Friščić and W. Jones, *J. Am. Chem. Soc.*, 2008, **130**, 7524–7525; (*b*) H. Deng, A. N. Gifford, A. M. Zvonok, G. Cui, X. Li, P. Fan, J. R. Deschamps, J. L. Flippen-Anderson, S. J. Gatley and A. Makriyannis, *J. Med. Chem.*, 2005, **48**, 6386–6392; (*c*) P. G. Jones, I. Dix and H. Hopf, *CSD Communication*, 2015, refcode QUNPAS; (*d*) E. F. Serantoni, L. Riva di Sanseverino and P. Sabatino, *Acta Crystallogr., Sect. B: Struct. Crystallogr. Cryst. Chem.*, 1980, **36**, 2473–2476; (*e*) D. E. Jeffries, J. O. Witt, A. L. McCollum, K. J. Temple, M. A. Hurtado, J. M. Harp, A. L. Blobaum, C. W. Lindsley and C. R. Hopkins, *Bioorg. Med. Chem. Lett.*, 2016, **26**, 5757–5764; (*f*) P. Tongwa, T. L. Kinnibrugh, G. R. Kicchaiahgari, V. N. Khrustalev and T. V. Timofeeva, *Acta Crystallogr., Sect. C: Cryst. Struct. Commun.*, 2009, **65**, o155–o159.

13 (*a*) O. Dumele, D. Wu, N. Trapp, N. Goroff and F. Diederich, *Org. Lett.*, 2014, **16**, 4722–4725; (*b*) H. S. Yathirajan, A. N. Mayekar, B. Narayana, B. K. Sarojini and M. Bolte, *Acta Crystallogr., Sect. E: Struct. Rep. Online*, 2007, **63**, o2196–o2197; (*c*) F. D. Cukiernik, A. Zelcer, M. T. Garland and R. Baggio, *Acta Crystallogr., Sect. C: Cryst. Struct. Commun.*, 2008, **64**, o604–o608; (*d*) Y. Çetinkaya, A. Menzek, E. Şahin and H. T. Balaydın, *Tetrahedron*, 2011, **67**, 3483–3489; (*e*) H. Xu, Q. Wang and Y. Guo, *Chem. – Eur. J.*, 2011, **17**, 8299–8303; (*f*) Y. Tang, R. Han, M. Lv, Y. Chen and P. Yang, *Tetrahedron*, 2015, **71**, 4334–4343; (*g*) Z. Zhang, L. Chang, S. Wang, H. Wang and Z.-Y. Yao, *RSC Adv.*, 2013, **3**, 18446–18452; (*h*) M. Chaabene, A. Khatyr, M. Knorr, M. Askri, Y. Rousselin and M. M. Kubicki, *Acta Crystallogr., Sect. E: Crystallogr. Commun.*, 2016, **72**, 1167–1170.

14 Similar bifurcated motifs have also been noticed in systems that have ortho-hydroxy and methoxy groups, for example in: (*a*) A. Carletta, M. Zbačnik, M. Van Gysel, M. Vitković, N. Tumanov, V. Stilinović, J. Wouters and D. Cinčić, *Cryst. Growth Des.*, 2018, **18**, 6833–6842; (*b*) A. Carletta, F. Spinelli, S. d'Agostino, B. Ventura, M. R. Chierotti, R. Gobetto, J. Wouters and F. Grepioni, *Chem. – Eur. J.*, 2017, **23**, 5317–5329.

15 (*a*) A. Verma, K. Tomar and P. K. Bharadwaj, *Cryst. Growth Des.*, 2019, **19**, 369; (*b*) R. Bhowal, S. Biswas, D. P. Adiyeri

 This journal is © The Royal Society of Chemistry 2020

Saseendran, A. L. Koner and D. Chopra, *CrystEngComm*, 2019, **21**, 1940; (*c*) H. Wang and W. J. Jin, *Acta Crystallogr., Sect. B: Struct. Sci., Cryst. Eng. Mater.*, 2017, **73**, 210.

16 (*a*) N. Bedeković, V. Stilinović, T. Friščić and D. Cinčić, *New J. Chem.*, 2018, **42**, 10584; (*b*) L. C. Roper, C. Präsang, V. N. Kozhevnikov, A. C. Whitwood, P. B. Karadakov and D. W. Bruce, *Cryst. Growth Des.*, 2010, **10**, 3710.

17 (*a*) S. L. James, C. J. Adams, C. Bolm, D. Braga, P. Collier, T. Friščić, F. Grepioni, K. D. M. Harris, G. Hyett, W. Jones, A. Krebs, J. Mack, L. Maini, A. G. Orpen, I. P. Parkin, W. C. Shearouse, J. W. Steed and D. C. Waddell, *Chem. Soc. Rev.*, 2012, **41**, 413–447; (*b*) T. Friščić and W. Jones, *Cryst. Growth Des.*, 2009, **9**, 1621–1637.

18 van der Waals radii according to: A. J. Bondi, *J. Phys. Chem.*, 1964, **65**, 441–451.

19 R. B. Walsh, C. W. Padgett, P. Metrangolo, G. Resnati, T. W. Hanks and W. T. Pennington, *Cryst. Growth Des.*, 2001, **1**, 165–175.

20 V. Nemec, L. Fotović, T. Friščić and D. Cinčić, *Cryst. Growth Des.*, 2017, **17**, 6169–6173.

Published on 10 agosto 2020. Downloaded on 09/10/2024 05:17:54.